



Hydroxylation and dechlorination of 3,3',4,4'-tetrachlorobiphenyl (CB77) by rat and human CYP1A1s and critical roles of amino acids composing their substrate-binding cavity

Yabu, Miku ; Haga, Yuki ; Itoh, Toshimasa ; Goto, Erika ; Suzuki, Motoharu ; Yamazaki, Kiyoshi ; Mise, Shintaro ; Yamamoto, Keiko ;...

(Citation)

Science of the Total Environment, 837:155848

(Issue Date)

2022-09-01

(Resource Type)

journal article

(Version)

Accepted Manuscript

(Rights)

© 2022 Elsevier B.V.

This manuscript version is made available under the CC-BY-NC-ND 4.0 license

<http://creativecommons.org/licenses/by-nc-nd/4.0/>

(URL)

<https://hdl.handle.net/20.500.14094/90009329>



Supporting Information

Hydroxylation and dechlorination of 3,3',4,4'-tetrachlorobiphenyl (CB77) by rat and human CYP1A1s and critical roles of amino acids composing their substrate-binding cavity

Miku Yabu^a, Yuki Haga^b, Toshimasa Itoh^c, Erika Goto^a, Motoharu Suzuki^b, Kiyoshi Yamazaki^a, Shintaro Mise^a, Keiko Yamamoto^c, Chisato Matsumura^b, Takeshi Nakano^d, Toshiyuki Sakaki^e, and Hideyuki Inui^{a,f,*}

^a Graduate School of Agricultural Science, Kobe University, 1-1 Rokkodaicho, Nada-ku, Kobe, Hyogo 657-8501, Japan

^b Hyogo Prefectural Institute of Environmental Sciences, 3-1-18 Yukihirocho, Suma-ku, Kobe, Hyogo 654-0037, Japan

^c Laboratory of Drug Design and Medicinal Chemistry, Showa Pharmaceutical University, 3-3165 Higashi-Tamagawagakuen, Machida, Tokyo 194-8543, Japan

^d Research Center for Environmental Preservation, Osaka University, 2-4 Yamadaoka, Suita, Osaka 565-0871, Japan

^e Department of Pharmaceutical Engineering, Faculty of Engineering, Toyama Prefectural University, 5180 Kurokawa, Imizu, Toyama 939-0398

^f Biosignal Research Center, Kobe University, 1-1 Rokkodaicho, Nada-ku, Kobe, Hyogo 657-8501, Japan

*Corresponding Author

Hideyuki Inui, Biosignal Research Center, Kobe University, 1-1 Rokkodaicho, Nada-ku, Kobe, Hyogo, 657-8501, Japan

E-mail: hinui@kobe-u.ac.jp, Telephone number: +81-78-803-5863

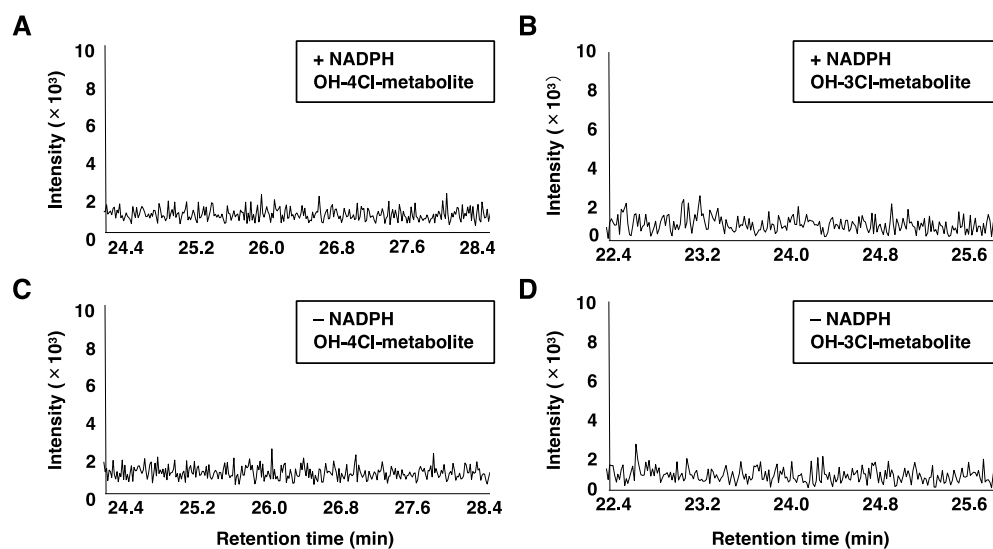


Fig. S1 Measurement of 3,3',4,4'-tetrachlorobiphenyl (CB77) metabolites produced by control microsomes. Vector control microsomes were incubated in the reaction mixture with 6.9 μM CB77 for 2 h. The extracted metabolites were quantified by performing high-resolution gas chromatography/high-resolution mass spectrometry after methylation. (A, B) Vector control with NADPH. (C, D) Vector control without NADPH.

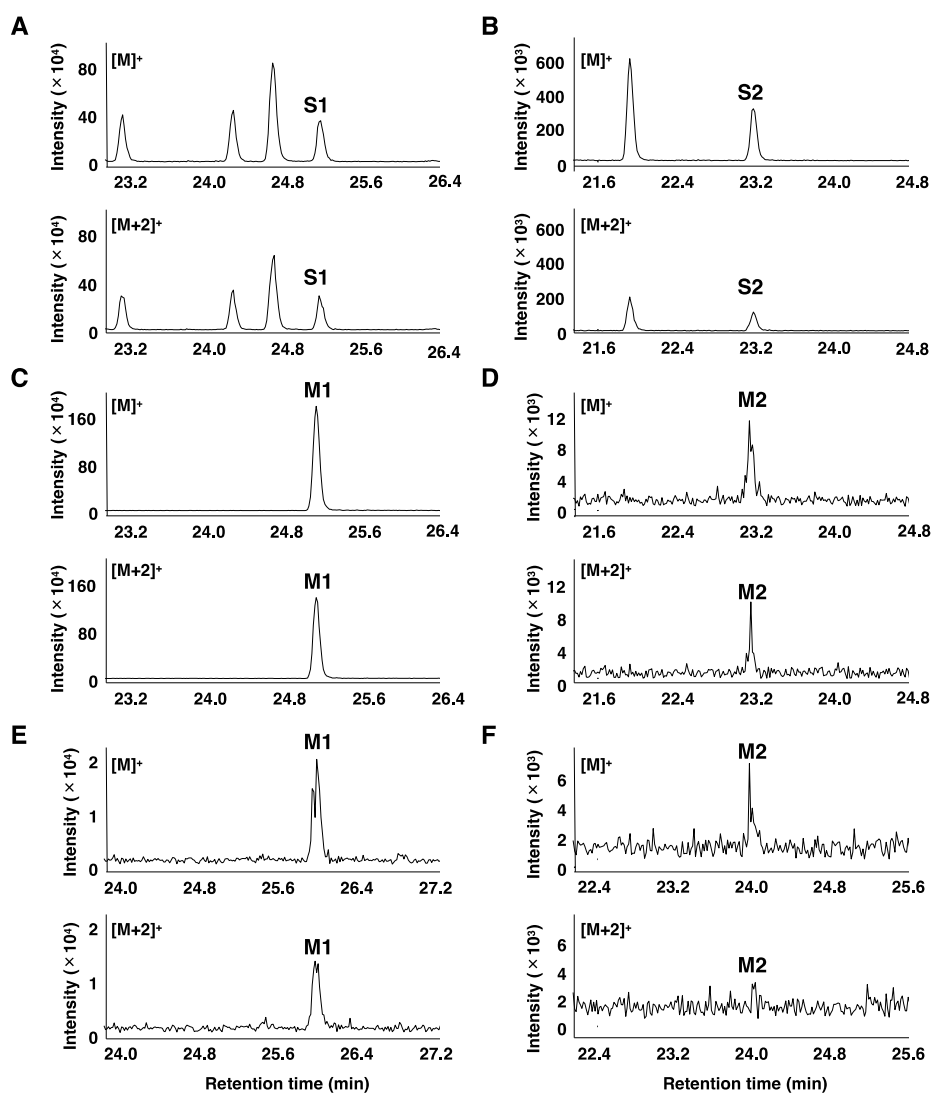


Fig. S2 Isotope ratios of methylated 3,3',4,4'-tetrachlorobiphenyl (CB77) metabolites produced by rat (C, D) and human (E, F) CYP1A1s. (A, B) Authentic standards: peak S1, 5-MeO-2,3',4,4'- or 4'-MeO-3,3',4,5'-tetrachlorobiphenyl; peak S2, 4'-MeO-3,3',4-trichlorobiphenyl. (C, D) Rat CYP1A1 with NADPH. (E, F) Human CYP1A1 with NADPH.

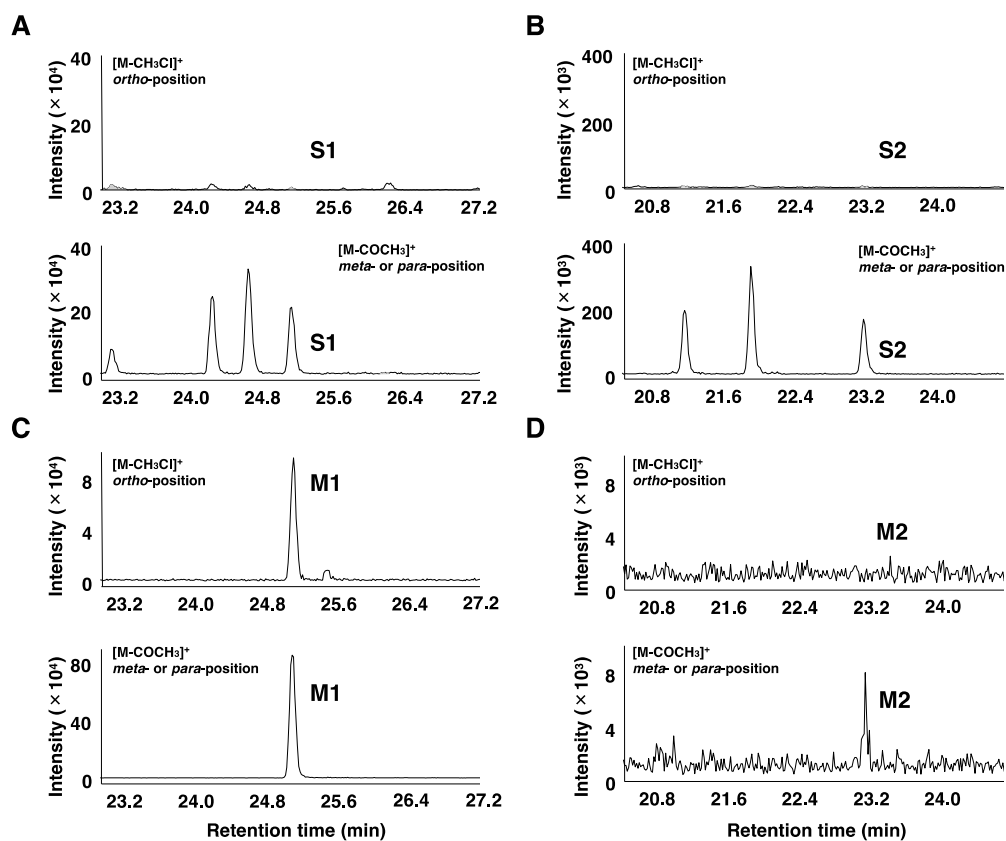


Fig. S3 Chromatograms of fragment ions from 3,3',4,4'-tetrachlorobiphenyl (CB77) metabolites. (A, B) Authentic standards: peak S1, 5-MeO-2,3',4,4'- or 4'-MeO-3,3',4,5'-tetrachlorobiphenyl; peak S2, 4'-MeO-3,3',4-trichlorobiphenyl. (C, D) Rat CYP1A1 with NADPH.

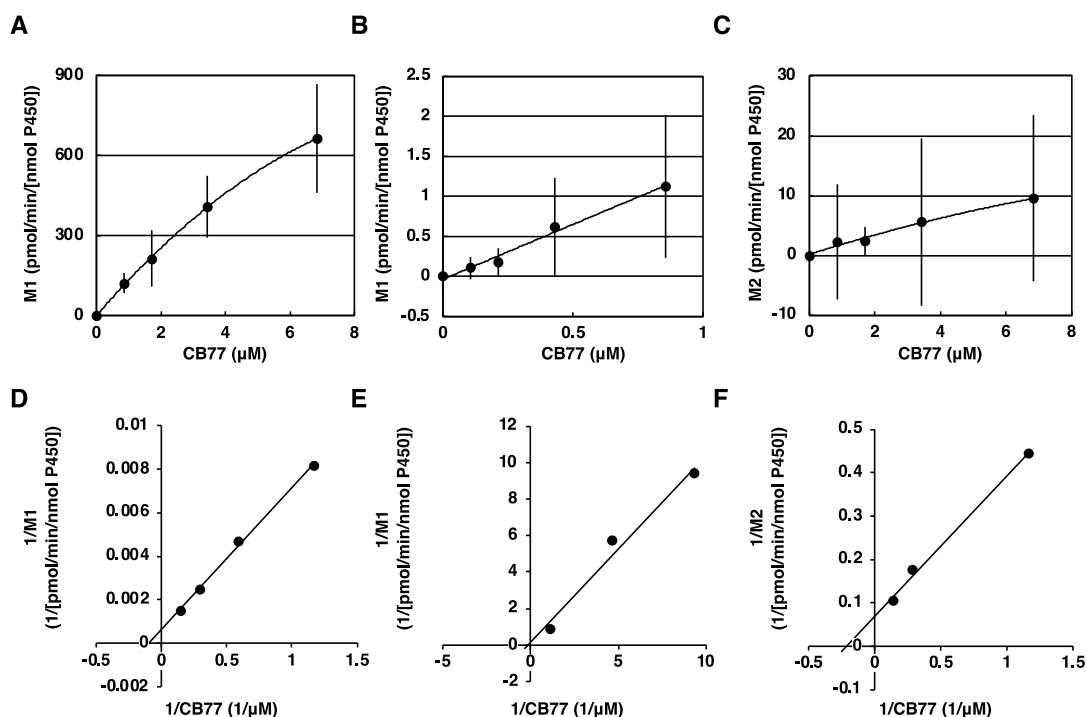


Fig. S4 Michaelis–Menten (A–C) and Lineweaver–Burk (D–F) plots of kinetics of CYP1A1s for hydroxylation of 3,3',4,4'-tetrachlorobiphenyl (CB77). Microsomes containing 80 nM of rat and human CYP1A1s were reacted with 0–6.9 and 0–0.86 μM CB77, respectively. The extracted metabolites were quantified by performing high-resolution gas chromatography/high-resolution mass spectrometry after methylation. All values are shown as the mean \pm standard deviation of five independent experiments. (A, D) M1 predicted as 4'-OH-3,3',4,5'-tetrachlorobiphenyl produced by rat CYP1A1. (B, E) M1 produced by human CYP1A1. (C, F) M2 identified as 4'-OH-3,3',4-trichlorobiphenyl produced by rat CYP1A1.

A		
Rat CYP1A1	352 CTTATC GCT AATGGCCAGAGCATGACTTTCAACCCAGACTCTGGACCGCTG 402	
	118 L I A N G Q S M T F N P D S G P L 134	
Rat CYP1A1 mutant	352 CTTATC TCT AATGGCCAGAGCATGACTTTCAACCCAGACTCTGGACCGCTG 402	
	118 L I S N G Q S M T F N P D S G P L 134	
Rat CYP1A1	901 AATGCCAATGTCCAGCTCTCAGATGATAAGGTCATTACGATTGTT TTT GAC 951	
	301 N A N V Q L S D D K V I T I V F D 317	
Rat CYP1A1 mutant	901 AATGCCAATGTCCAGCTCTCAGATGATAAGGTCATTACGATTGTT CTT GAC 951	
	301 N A N V Q L S D D K V I T I V L D 317	
B		
Human CYP1A1	301 GATGATTTCAAGGGCCGGCCGACCTCTACACCTTCACCCTCATC AGT AAT 351	
	101 D D F K G R P D L Y T F T L I S N 117	
Human CYP1A1 mutant	301 GATGATTTCAAGGGCCGGCCGACCTCTACACCTTCACCCTCATC GCT AAT 351	
	101 D D F K G R P D L Y T F T L I A N 117	
Human CYP1A1	901 CAGCTGTCAGATGAGAAGATCATTAAACATCGTC TTG GACCTCTTTGGAGCT 951	
	301 Q L S D E K I I N I V L D L F G A 317	
Human CYP1A1 mutant	901 CAGCTGTCAGATGAGAAGATCATTAAACATCGTC TTT GACCTCTTTGGAGCT 951	
	301 Q L S D E K I I N I V F D L F G A 317	

Fig. S5 Mutation of DNA sequences of rat (A) and human (B) *CYP1A1*s and deduced amino acid sequences. Red codons and amino acids are mutated sequences.

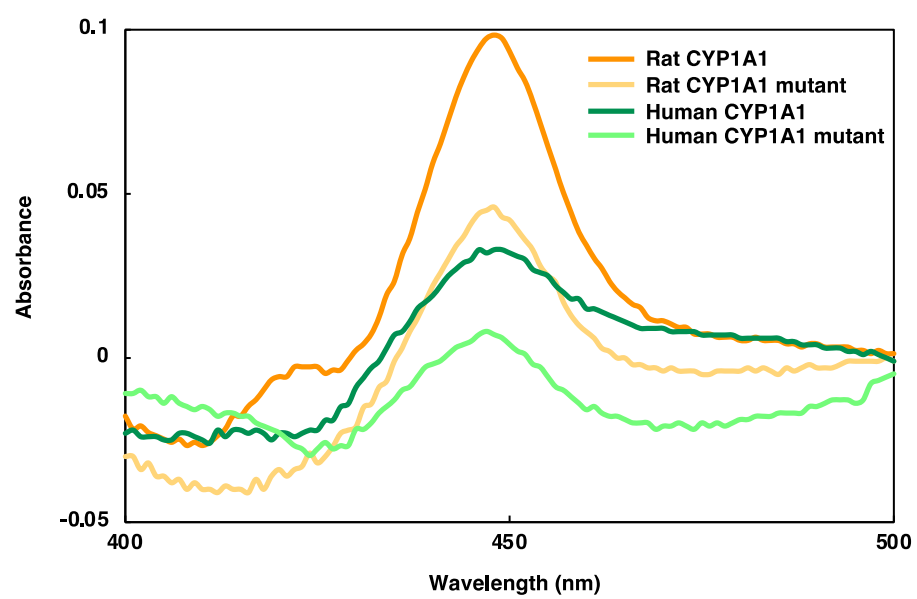


Fig. S6 Reduced difference CO spectra of rat and human CYP1A1s and their mutants.

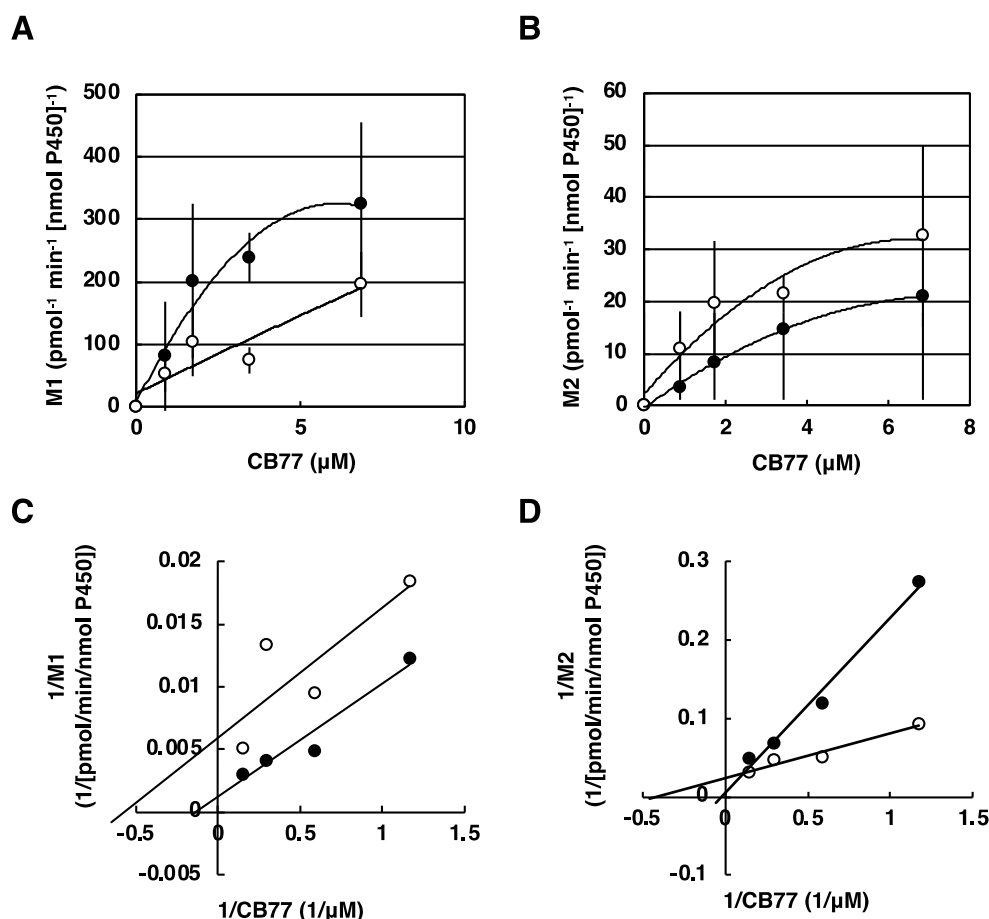


Fig. S7 Michaelis–Menten (A, B) and Lineweaver–Burk (C, D) plots of kinetics of rat CYP1A1 and its mutant for hydroxylation of 3,3',4,4'-tetrachlorobiphenyl (CB77). Microsomes containing 80 nM of rat CYP1A1s and its mutant were reacted with 0–6.9 μM CB77. The extracted metabolites were quantified by performing high-resolution gas chromatography/high-resolution mass spectrometry after methylation. All values are shown as the mean ± standard deviation of five independent experiments. (A, C) M1 predicted as 4'-OH-3,3',4,5'-tetrachlorobiphenyl produced by rat CYP1A1 and its mutant indicated by closed and open circles, respectively; (B, D) M2 identified as 4'-OH-3,3',4-trichlorobiphenyl produced by rat CYP1A1 and its mutant indicated by closed and open circles, respectively.

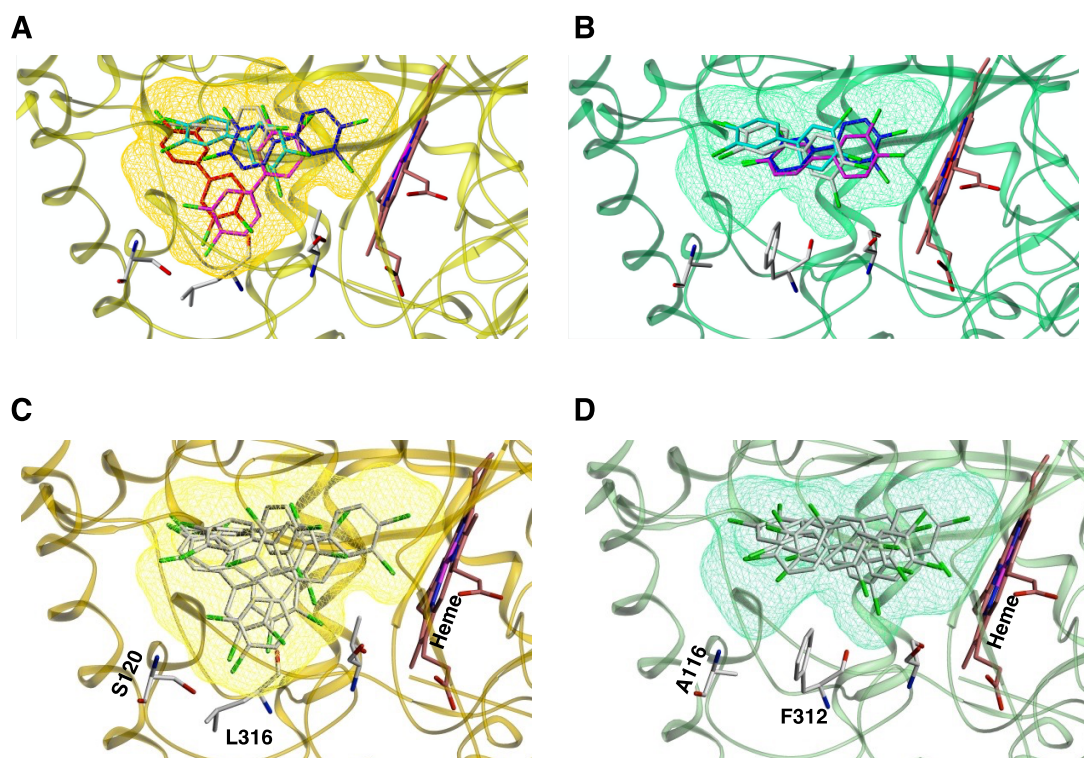


Fig. S8 Docking models of rat (A) and human (B) CYP1A1 mutants with 3,3',4,4'-tetrachlorobiphenyl (CB77). Connolly channel surfaces of the cavities are displayed using a colored mesh. (A, B) Representative orientations of CB77 in the substrate-binding cavity of rat (five orientations) and human (four orientations) CYP1A1 mutants; (C, D) Conformations of CB77 close to the heme iron in rat (six conformations) and human (five conformations) CYP1A1 mutants.

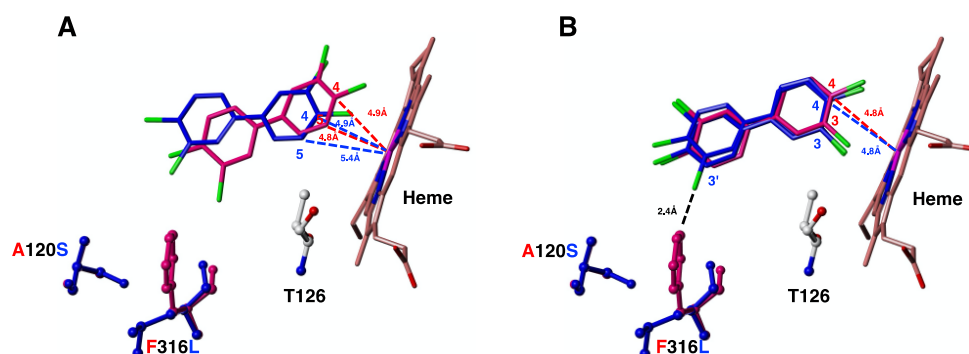


Fig. S9 Conformations of 3,3',4,4'-tetrachlorobiphenyl (CB77) to produce the metabolites M1 and M2 by rat CYP1A1 and its mutant. (A) Difference in conformations to produce M1, predicted as 4'-OH-3,3',4,5'-tetrachlorobiphenyl, between rat CYP1A1 and its mutant. (B) Difference in conformations to produce M2, identified as 4'-OH-3,3',4-trichlorobiphenyl, between rat CYP1A1 and its mutant. CB77 structures shown in red and blue represent CB77 docked to rat CYP1A1 and its mutant, respectively. The amino acids in red and blue represent rat CYP1A1 and its mutant, respectively.

Table S1 Sequences of the primers used in this study.

Primer	Sequence
t946c as	5'-CTCCAAAGAGGTCAAGAACAATCGTAATGACCTTATCATCTGAG-3'
g358t as	5'-CATGCTCTGGCCATTAGAGATAAGTGTGAAGCTGT-3'
g936t as	5'-GCTCCAAAGAGGTCAAAGACGATGTTAATGATCTTCTCATC-3'
a346g g347c as	5'-GGACATGCTCTGACCATTAGCGATGAGGGTGAAGGTGTAC-3'

Table S2 7-Ethoxycoumarin *O*-deethylation activity of CYP1A1s and its mutants.

P450	P450 content ¹	7-Ethoxycoumarin <i>O</i> -deethylation ^{2,3}
Rat CYP1A1	110	31.5 ± 1.46
Rat CYP1A1 mutant	24.2	27.8 ± 1.33**
Human CYP1A1	15.8	0.544 ± 0.0470
Human CYP1A1 mutant	7.61	1.2 ± 0.164**

¹ pmol/mg; ² nmol/min/(nmol P450); ³ All values are mean ± standard deviation of five independent experiments. **, $p < 0.01$ by Student's *t*-test (wild-type)